FATIGUE FAILURE MECHANISM OF REINFORCED CONCRETE BRIDGE DECK SLABS

Kiyoshi Okada, Kyoto University
Hirokazu Okamura, Osaka Institute Technology
Keiichiro Sonoda, Osaka City University

The aim of the paper is to clarify the fatigue failure mechanism of reinforced concrete slabs under moving wheel loads. Seven slabs with full scale dimensions were tested under static load, central pulsating loads, and moving pulsating loads. To investigate deflection characteristic and reserve fatigue strength of cracked slabs subjected to actual traffic loads, especially, four test slabs were sawn out from two distressed bridge decks. Experimental findings were mainly as follows: rubbing together of crack faces due to the repeatedly moving loads eventually produced a slit with a narrow opening in the cracked section; the formation of the slit reduced both flexural and shearing rigidities of the slab; if rain water were poured into the cracked section, the reductions of these rigidities were remarkably accelerated and caused the slab surface to collapse prematurely. Three-dimensional stress analysis in the vicinities of cracks predicted their penetration through the entire depth of the slab. It was found that the process of the penetration consisted of two stages: the first stage was a growth of flexural cracks occurring at the bottom surface of the slab, beneath the wheel load, and the second stage was a progression of twisting cracks occurring at the top surface, when the wheel load had moved away.

Introduction

The design code for reinforced concrete bridge deck slabs in Japan follows an allowable stress method based upon the thin elastic plate bending theory, which has been supposed to lead to conservative results. During the past decade, however, many instances of damage or collapse of deck slabs have been reported in Japan. To examine direct or indirect causes for such damage or collapse, some tests of model and prototype slabs have been carried out under both static and pulsating loads, but these test results merely indicated that the slabs had load-carrying capacities several times greater than the design loads (1,2). On the other hand, from field observations on actual damaged deck slabs, the effects of rolling and moving wheel loads on fatigue of deck slabs appear to be highly significant. However, such effects have not been considered in previous tests.

The aim of this study is to clarify both experimentally and theoretically the fatigue strength and the failure mechanism of reinforced concrete deck slabs under moving wheel loads. Seven slabs with full-scale dimensions were tested under static, pulsating and moving pulsating loadings. In order to investigate reserve fatigue strengths and durabilities of cracked slabs under repeatedly moving loads, some of the test specimens were sawn out from two distressed bridge deck slabs which had been subjected to the traffic loads of 20 - 50 thousand cars a day over a period of 8 to 10 years. The other specimens were virgin slabs fabricated to the same specification as for the old slabs.

An analysis based upon three-dimensional elasticity of a model slab with grid-like cracks was made to investigate the distribution of stresses near the cracks due to moving loads and to clarify the process of crack growth through the entire depth of the slab, under the action of alternate transverse and twisting shearing stresses.

Description of Specimens and Tests

Details of the test specimens are given in Table 1. The specimens marked " O " were sawn out from the two distressed bridge decks. The cracking pattern of one of these specimens is illustrated in Fig.1, in which the existence of numerous cracks of widths 0.05 - 0.2 mm at the bottom surface of the slab, some of which penetrate to the top surface are apparent. The specimens marked " N " mean full-scale virgin slabs made for these tests. All specimens also include top reinforcement amounting to about 50 % of the bottom reinforcement indicated in Table 1. The reinforcement consists of round steel bars with diameters 16 mm in the longitudinal direction and 13 mm in the transverse direction. These specimens have standard depth and reinforcement in accordance with the Japanese code.

The test setup is shown in Fig.2. The slabs were supported rigidly along their longer edges and elastically on steel beams with H-sections along their shorter edges so as to obtain variations of

bending moments comparable to those in actual bridge deck slabs which are supported on longitudinal steel girders. To ensure bond strength of reinforcing bars in the sawn-out slabs, ends of the bars were welded to anchorage steel plates placed on edge-sides of the slabs.

Load was applied on a 20 x 50 cm^2 rectangular area corresponding to one rear wheel load specified by the code. Two types of loading procedures were used: static or pulsating loads applied at center of slab, and pulsating loads transferred stepwise and cyclically on several different points as shown in Fig.4. The number of cycles of pulsating load per point was in the range from 0.2 x 10^4 to 1.0 x 10^4. The latter type was regarded as a simulation of moving wheel loads. The movement of loading point was carried out by sliding stepwise the slabs in the longitudinal direction, and by changing in the transverse direction the support-point of the lever arm sustaining a pulsating load from an actuator. The pulsating load was of sinusoidal wave form and frequencies ranged from 4 Hz to 5 Hz. The intensity of the load was varied for different tests in the range between 108 kN corresponding to one rear wheel load including impact load specified by the code and 245 kN of the maximum capacity of the testing machine used. Loading sequences for the various specimens are shown in Fig.3.

Observation of Crack Propagation

In the central pulsating loading test of the virgin slab N_2, radial cracking patterns developed at the bottom surface of the slab, spreading from the loading point. Crack propagation was slow, and nearly ceased after one hundred thousand cycles of a load successively higher than previous maximum load. Initial cracks occurred beneath a loading point and then extended along the principal moment trajectory. In the moving pulsating loading test of the virgin slab N_3, on the other hand, the cracking pattern had a grid-like form similar to that of the old slab as shown in Fig.1. Movement of the loads sequentially changed the principal moment directions, and consequently, the cracking spread over the entire lower surface of the slab. In the slab N_3, the grid-like cracking pattern was essentially completed after 200 x 10^4 cycles of loading and 50 cycles of movement, in which one cycle of movement consisted of the pulsating loadings of five different points aligned as shown in Fig.4.

The relationships between the characteristics of the cracked surface and the number of cycles of the pulsating load obtained in specimen N_3 are indicated in Fig.5. The crack density, which is defined here as the total length of surface cracks per unit area, becomes stationary after a finite number of cycles. Namely, new cracks occur severely only at the initial stage of loading. On the other hand, by the actions of alternate compression and twisting due to sequential and repeated movements of loads, the crack faces are clapped together and rubbed against each other, and consequently the crack faces are worn away and then a slit with a narrow opening is formed in the cracked section. This was confirmed in the test through observation of sequential falling of fine concrete powder from crack openings. This will also be supported by field observations that in actual damaged deck slabs so large plastic deformations did not occur, in spite of the existence of numerous cracks with large residual widths.

The formation of such a slit impairs the continuity of flexural rigidity and also causes a remarkable reduction of shearing strength mainly relying upon interlocking of the aggregate particles. A discontinuity of flexural rigidity is shown in Fig.6, where cracks beneath the load open widely but other cracks in a slightly remote position from the load contrastedly close until widths remaining under no loading vanish, and the behaviours of these cracks greatly differ from the shape of the moment influence line predicted by the homogeneous elastic plate theory. Furthermore, such a discontinuity will produce alternate stresses of compression and tension on the upper side of the cracked section with the movement of the load and then will eventually result in penetration of cracks across the entire depth. In specimen N_3, such a fully penetrating crack was detected in the longitudinal direction after 490 x 10^4 cycles of loading and 190 cycles of movement of the load with 226 kN as a maximum, corresponding to about twice the design load (see crack B in Fig. 6). The cycles of movement of the load were greatly restricted in number because with the loading equipment used the movements were carried out manually. Therefore, more cycles of load movement which would be encounted in actual bridge decks could be assumed to reduce considerably the load intensity causing full penetration cracking. Further discussion on full penetration cracking will be described in a subsequent section.

Stresses of Reinforcing Bars

Table 2 shows a comparison of observed strains and theoretical ones of longitudinal bottom reinforcing bars in cracked sections beneath the load. The theoretical strains are derived from the conventional elastic equation neglecting the strength of tensile concrete under a moment obtained by the elastic plate bending theory. It can be concluded from these results that the stress intensity of reinforcing bars is sufficiently small in the initial stage of cracking and does not exceed, in the state of extensive cracking, the value predicted by the conventional elastic equation.

Deflection Characteristics

Fig.7 shows load-central deflection curves of specimens N_1, O_1, N_2 and O_2. The deflections of the slabs with slight cracks may be estimated, in the ranges below or near the design load, by the isotropic elastic plate theory with consideration of the flexural rigidity of entire slab depth, and those of the impaired slabs with a number of fully penetrating cracks as shown in Fig.1 may be predicted well by the orthotropic elastic plate theory with the rigidities of only compressive concrete and tensile reinforcement. Fig.8 indicates how the central deflection under constant load of 108 kN corresponding to design load grows with the number of cycles of loading. It seems that the increase of deflection under the central loading is very slow but deflection under moving loading gradually increases.

In field observations of actual damaged bridge decks it often has been seen that rain water comes through concrete slabs along cracks in asphalt pavement, and a solution of lime causes precipitation of calcium carbonate at the lower sides of the cracked sections of the slabs. To examine the effect of the water infiltrated into the cracked

sections on slab failure under moving pulsating loading, specimens O_3 and O_4 were tested in a water-saturated state which was obtained by ponding water on the upper surface of the slab. It is clearly shown that water infiltrated into cracks remarkably influences increase of deflection. This is probably due to the fact that water infiltrated into cracks oozes out the fine powder of crushed concrete from the crack openings by virtue of vibrating action of the slab, and the enlargement of crack width consequently induces accelerative reductions of both flexural and shearing rigidities.

Collapse Load and Fatigue Failure Mechanism

It is well known that slabs loaded at the center collapse in punching shear modes. Some specimens in the tests collapsed eventually due to punching shear of concrete after precedence of partial flexural failure. The values of collapse loads of the specimens are shown in Table 3. The collapse load of the virgin slab N_1 under central static-loading agreed well with the value predicted by the punching shear failure formula presented by Kakuta et al. (3). In the old slab O_1 distressed due to travelling of actual traffic loads, the collapse load in the static test seemed to be somewhat reduced by the influence of the existence of extensive cracks, but still it was very large in comparison with the design load. The old slab O_2 under central pulsating loading collapsed due to fatigue fracture of tensile reinforcing bars at the maximum load 245 kN equal to 2.3 times the design load. However, the virgin slab N_2 did not collapse under the same load.

On the other hand, it was clearly recognizable that water infiltrated into the cracked sections caused the premature collapse of the slab. Specimen O_3 collapsed under maximum load of 167 kN and at 530×10^4 cycles of loading, the specimen having been loaded in a wet condition after 475×10^4 cycles in a dry condition. Specimen O_4 which was tested from the start in a wet condition under a constant load of 108 kN corresponding to the design load collapsed at 250×10^4 cycles of loading. The collapse mechanism of a slab saturated with water proceeded as follows: when the deteriorated slab with many fully penetrating cracks was saturated with water, the crushed concrete powder existing in the cracks was changed into a mud-like paste and flowed out from the crack openings by virtue of the pumping effect due to vibration of the slab. Consequently, the crack openings were rapidly enlarged with the repetitions of loading and the shear resistance of the slab was reduced remarkably. After falling of small concrete fragments from the cracked sections followed by peeling off of the concrete covering the bottom reinforcing bars, the upper surface of the slab eventually caved in and collapsed.

Theoretical Consideration

To research further the process of full penetration of cracks into flexural compression side, which was detected in the previous experiment, a three-dimensional stress analysis for the concrete near tip of flexural crack and the reinforcing bars was carried out under the assumptions: concrete and reinforcing bars were of isotropic elastic material; tensile and shearing stresses were not transmitted through the surface of flexural cracks; dowel effects of reinforcing bars were neglected; reinforcing bars were perfectly bonded; the cracking pattern was of a grid-like form and spacing of cracks was about equal to slab depth. Further, to confirm a possibility of the failure of concrete due to such fully penetrating cracks in a bridge deck slab, a two-dimensional bending analysis for a one-way spanning slab was also carried out, and by the combination of results of this and those of three-dimensional analysis the range of principal tensile stress acting in concrete throughout the slab under moving wheel loads was examined.

The method of three-dimensional analysis here belongs to an integral equation method, described fully in the previous papers (4,5), which is developed by superposing the solutions of Mindlin's first and second problems and by using the collocation method. The characteristic of the method is that an objective slab containing a part with variable rigidity due to cracks and reinforcements is cut out from a semi-infinite elastic solid, by replacing the effect of deviation from uniform rigidity by application of equivalent self-equilibrating body forces.

A slab model for numerical investigations by the three-dimensional analysis was simplified, as shown in Fig.9, which had the following properties: all edges of the slab were simply supported; aspect ratio, $b/a=1.5$; depth of cracks, $h_t=0.7h$; spacing of cracks, $e=h$; loaded area, $u \times v = 0.039\, a^2$; Poisson's ratio of concrete, $\nu=1/6$; ratio of elastic moduli of steel and concrete $=10$; ratio of bottom reinforcement $=1.0$ %. The value $h_t=0.7h$ was taken from the assumption that flexural cracks would prematurely proceed from bottom face to the neutral plane determined by the conventional formula derived from neglecting the strength of tensile concrete and using Bernoulli's assumption.

Fig.10 shows distributions of the normal stresses in the compressive domain of the cracked section beneath the applied load. The results are almost the same as those by the conventional formula under moment calculated by the elementary plate bending theory.

Fig.11 shows distributions of the normal stress, σ_x, in concrete along the entire depth of the sections b - f as marked in Fig.9. Remarkable differences in the shapes of stress distributions are seen between cracked and uncracked sections, but the intensities of compressive stresses occurring at the top surface of each section are not different between them. Fig.12 shows variation of the tensile stress, σ_{sx}, acting in a reinforcing bar between cracked sections b - g. In this figure, it should be noted that the intensity of σ_{sx} in the cracked sections becomes large in comparison with that in the uncracked sections, but the maximum intensity is nearly equal to the values predicted by the conventional formula mentioned above.

On the other hand, distributions of transverse shearing stress, τ_{yz}, along the depth of compressive concrete in the cracked sections near the applied load are indicated in Fig.13. As the distributions of τ_{yz} are of nearly triangular shape, the intensities of it may be predicted well by assuming a linear distribution of the resultant shearing force, Q, which can be obtained by the elementary plate bending theory, as shown by the dotted lines in Fig.13.

Then, since the other stress components, except τ_{yz} at the crack tip which is nearly on the neutral plane are sufficiently small in comparison with τ_{yz}, the maximum principal tensile stress, σ_{pl}, due to the above stress concentration will amount to

Table 1. Details of specimens, material properties, and loadings.

Specimens	Sizes (m) (W) (L) (T)	Bottom Reinforcement (%) (Long.) (Trans.)	Strength of Conc. (MN/m^2)	Strength of Reinfct. Yield/ Ultimate (MN/m^2)	Type of Loading
N_1	2.5 x 3.8 x 0.18	1.3 / 0.5	25.0	274.7 / 454.2	Static
N_2	2.5 x 3.8 x 0.18	1.3 / 0.5	29.5	274.7 / 454.2	Central pulsating
N_3	2.5 x 3.8 x 0.18	1.3 / 0.5	31.4	274.7 / 454.2	Moving pulsating
O_1	2.5 x 3.8 x 0.18	1.3 / 0.5	31.7	323.7 / 461.1	Static
O_2	2.5 x 3.8 x 0.18	1.3 / 0.5	31.7	323.7 / 461.1	Central pulsating
O_3	1.8 x 2.7 x 0.17	1.1 / 0.4	40.8	318.8 / 438.3	Moving pulsating
O_4	1.8 x 2.7 x 0.17	1.1 / 0.4	40.8	318.8 / 438.3	Moving pulsating

Table 2. Tensile strains of reinforcing bars under central load 108 kN.

Specimens	Number of Cycles	Measured Values	Theoretical Values
N_1	Static	140×10^{-6}	381×10^{-6}
N_2	100	95×10^{-6}	381×10^{-6}
	4×10^5	115×10^{-6}	381×10^{-6}
N_3	1×10^4	110×10^{-6}	381×10^{-6}
	2×10^5	135×10^{-6}	381×10^{-6}
	5×10^5	175×10^{-6}	381×10^{-6}
	1.5×10^6	180×10^{-6}	381×10^{-6}
O_3	1	320×10^{-6}	441×10^{-6}
	1×10^4	360×10^{-6}	441×10^{-6}
	1×10^5	375×10^{-6}	441×10^{-6}
	5×10^5	420×10^{-6}	441×10^{-6}
	2×10^6	400×10^{-6}	441×10^{-6}

Figure 1. Cracking pattern of a distressed slab sawn out from bridge deck.

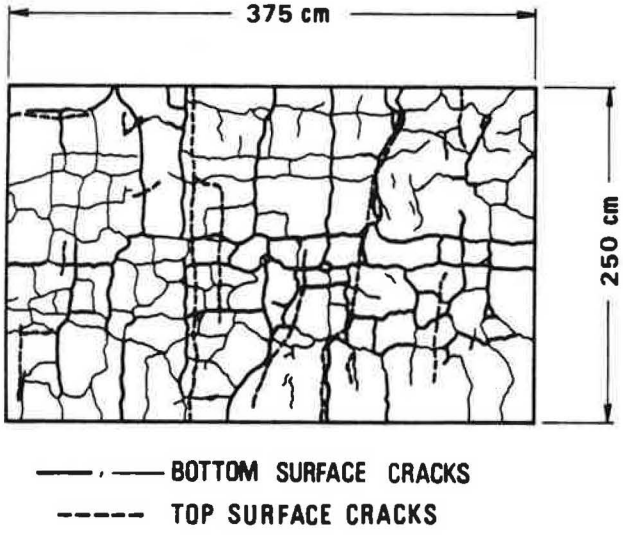

Table 3. Collapse loads.

Specimens	Collapse Loads (kN)	Total Number of Cycles	Remarks
N_1	626	Static	Calculated punching shear load 647 kN
N_2	No collapse	230×10^4	Maximum applied load 245 kN
N_3	No collapse	513×10^4	Maximum applied load 226 kN
O_1	526	Static	Calculated punching shear load 736 kN
O_2	245	275×10^4	Fracture of bottom reinforcing bars
O_3	167	526×10^4	No fracture of reinforcing bars
O_4	108	256×10^4	No fracture of reinforcing bars

Figure 2. Test setup.

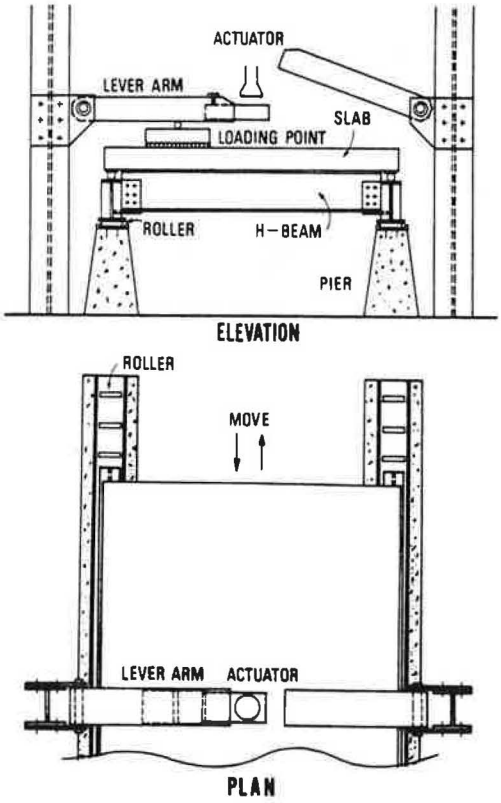

Figure 3. Loading sequences for each specimen.

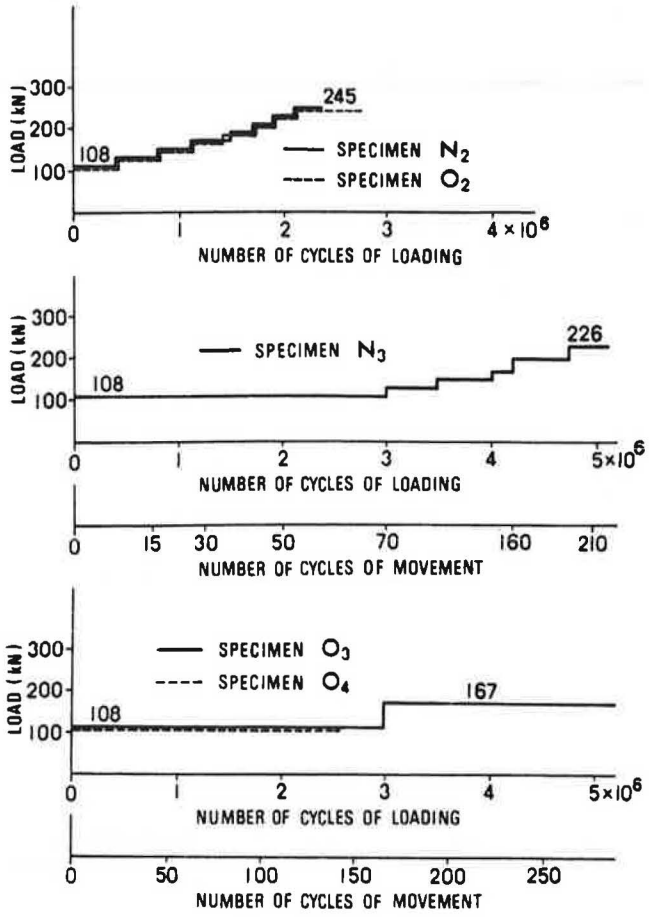

Figure 4. Sequence of movement of load.

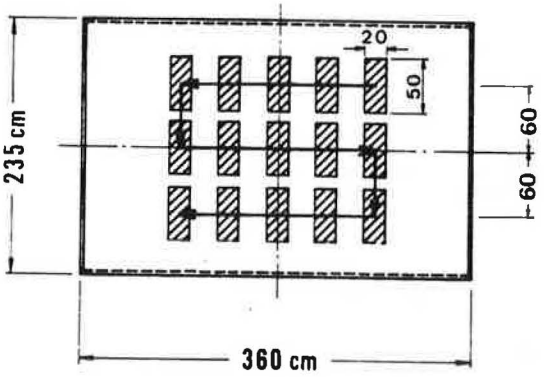

Figure 5. Characteristics of cracked surface of virgin slab related with cycles of moving pulsating loading.

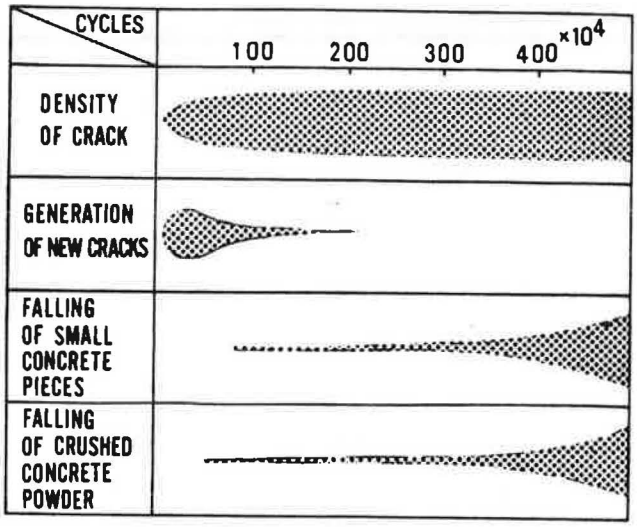

Figure 6. Relation between crack widths and location of loading point along transverse center line, in specimen N_3.

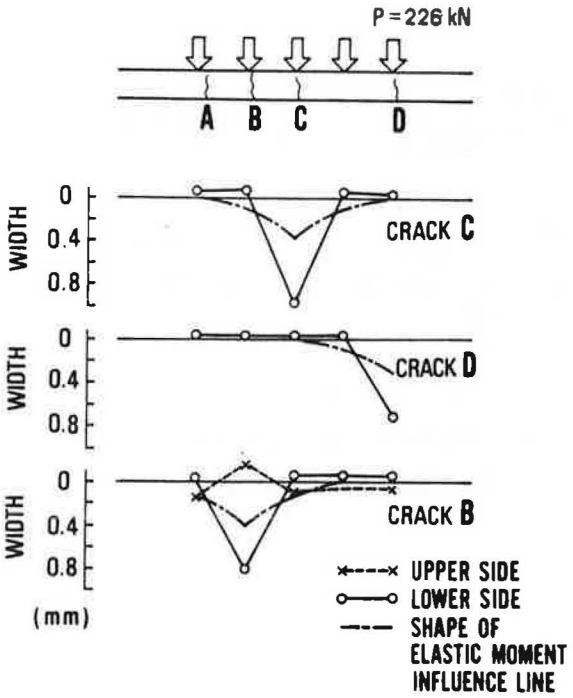

Figure 7. Load-deflection curves under central static or pulsating loadings.

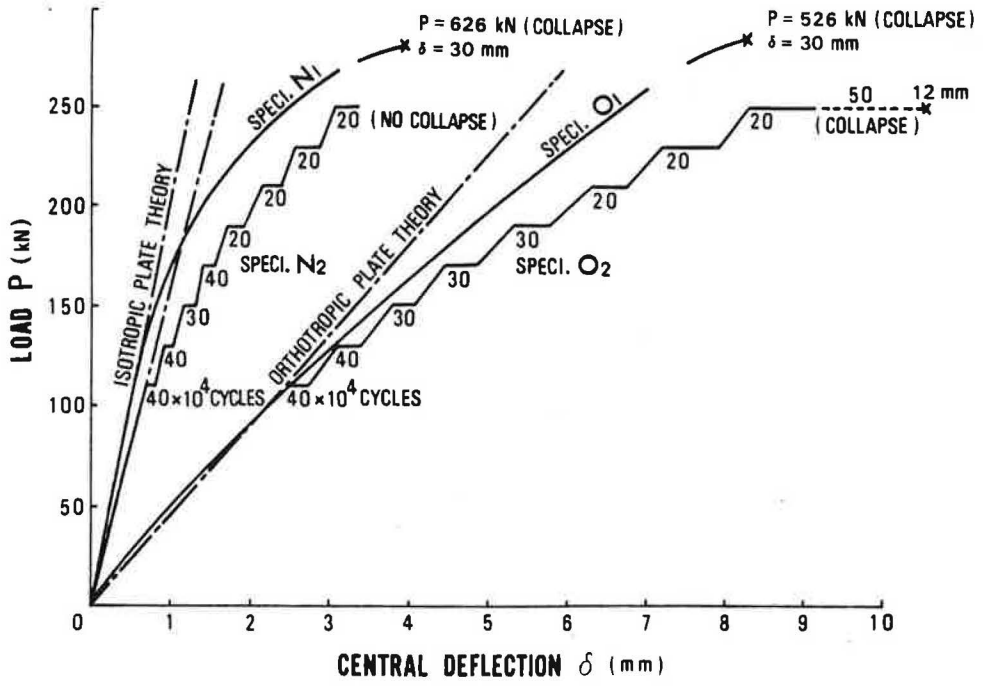

Figure 8. Relationships between growth of central deflection and cycles of loading under 108 kN.

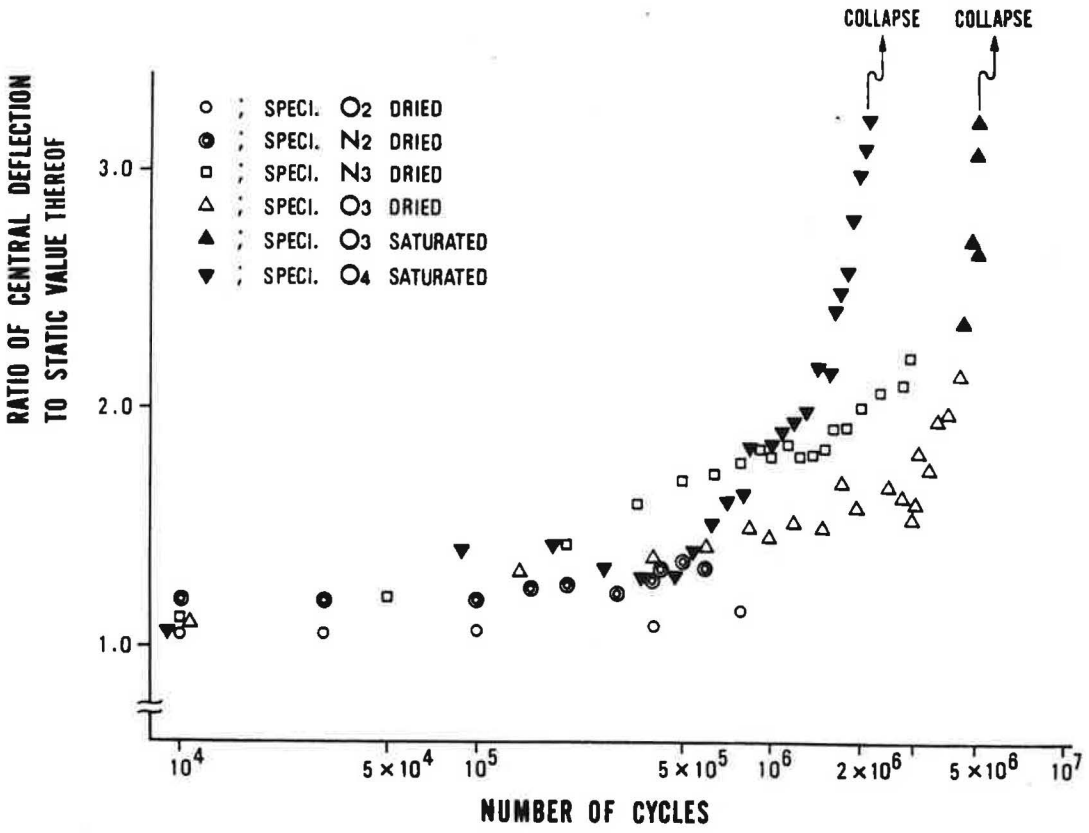

Figure 9. Model slab for numerical investigation.

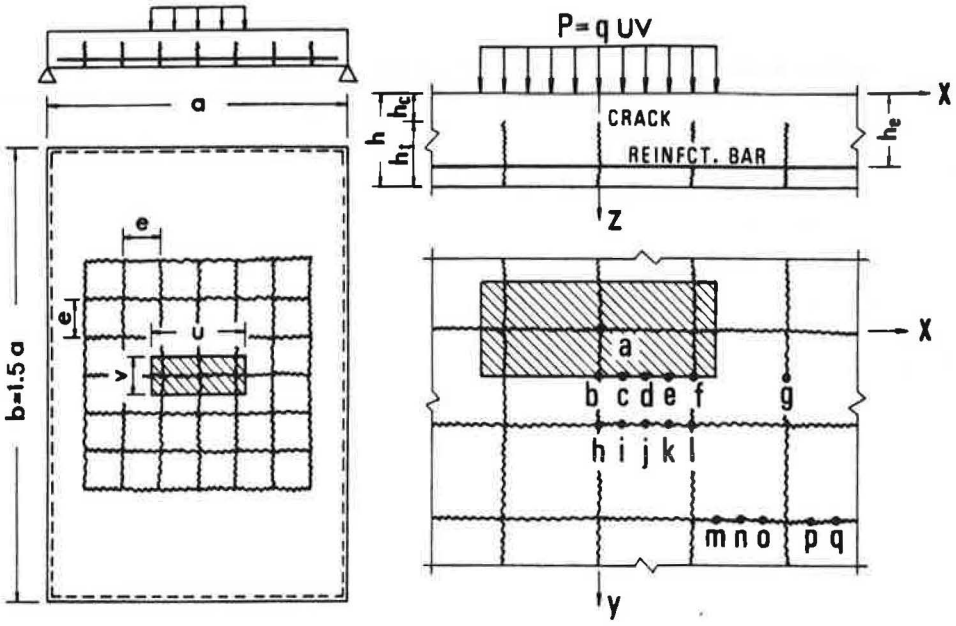

Figure 10. Variations of normal stresses in compressive domain.

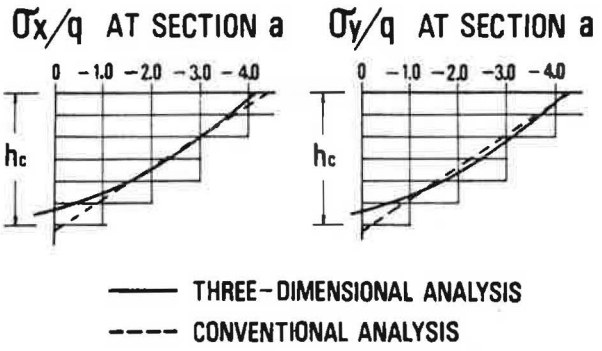

Figure 12. Variation of axial stress σ_{sx}/q in reinforcement.

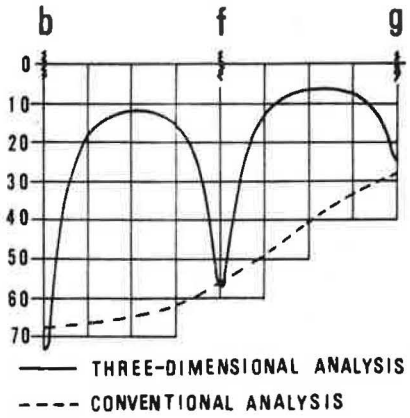

Figure 11. Variations of normal stress σ_x/q in concrete in cracked and uncracked sections.

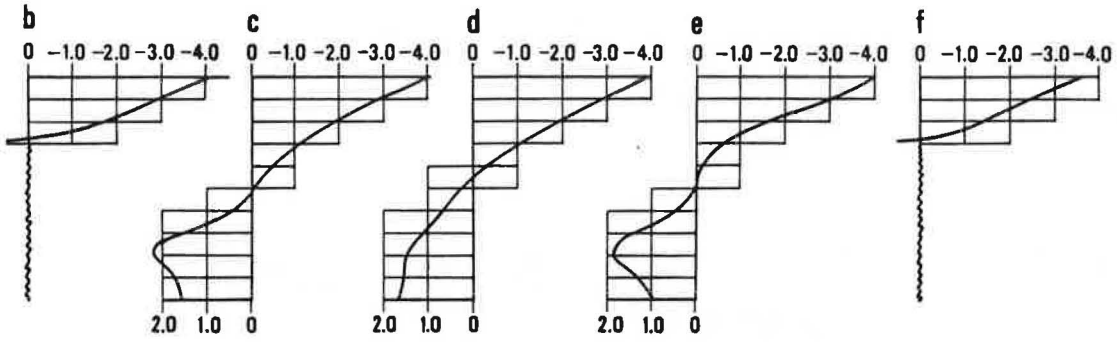

Figure 13. Variations of transverse shearing stress τ_{yz}/q in compressive domain.

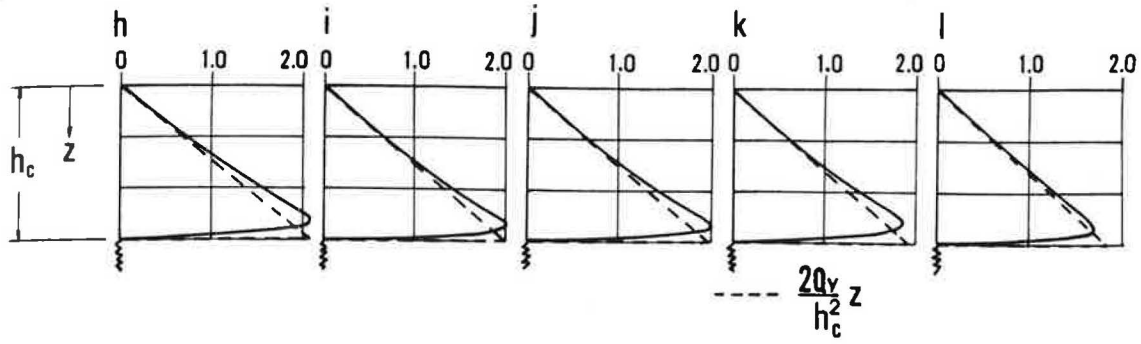

Figure 14. Variations of horizontal shearing stress τ_{xy}/q in compressive domain.

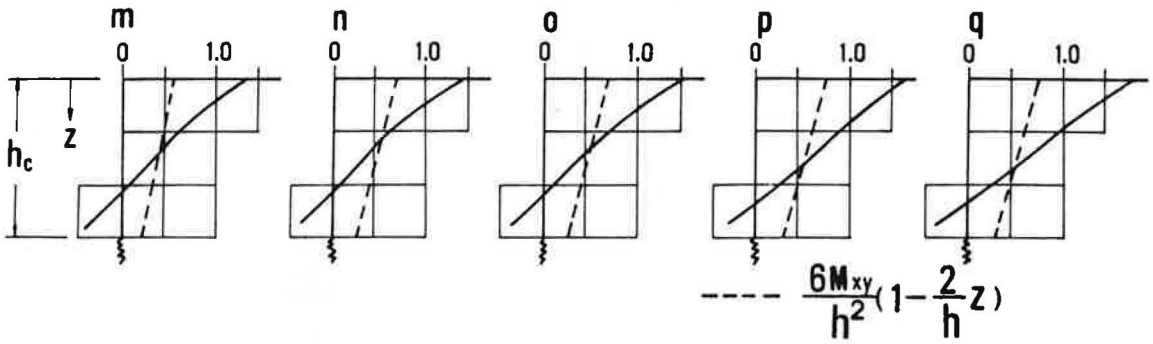

Figure 15. Distribution of transverse shearing forces along periphery of loaded area.

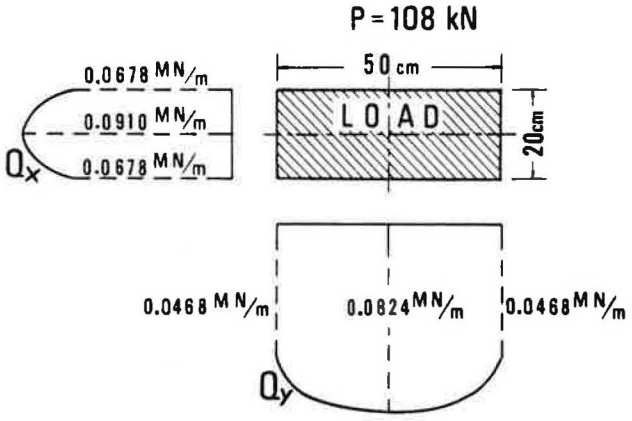

Figure 16. Contour line of twisting moment in a simply supported one-way slab under two rear wheel loads.

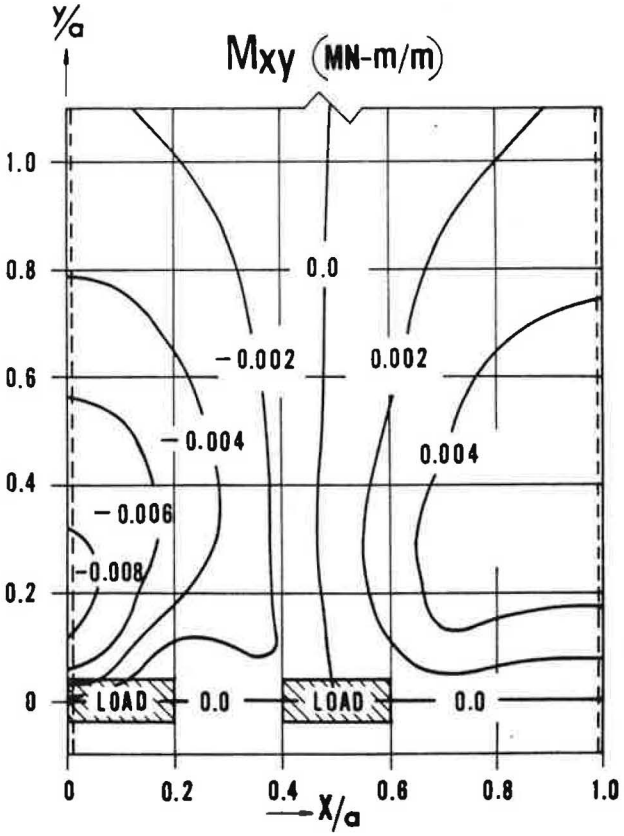

$$\sigma_{p1} \doteqdot 2.0 \frac{Q}{h_c} \quad (1)$$

in which h_c is depth of compressive concrete.

As severe intensity of Q will occur along the periphery of the loaded area, the distribution of Q along that periphery is examined by the plate bending theory, as shown in Fig.15, which is calculated for a one-way slab with the span, 250 cm, considered as an actual bridge deck, under the central load, 108 kN, corresponding to one rear wheel load as specified by the Japanese code. Substituting the maximum value of Q given by Fig.13 into eq.(1) under the assumption, h_c=6 cm, the intensity of tensile stress at the tip of a flexural crack reaches to 3.0 MN/m^2, which is considered to be larger than the tensile fatigue strength of plain concrete. Thus, if shear resistances of the surfaces of flexural cracks produced prematurely in a bridge deck slab are sufficiently reduced due to repeated traffic loads, as the previous experimental observation pointed out, then, a further progression of flexural cracks to the compression side becomes possible, but such cracks can not extend to the top surface of the slab, because large flexural compressive stresses are in existence near the top resulting from application of finite bending moment.

On the other hand, Fig.14 indicates distributions of the horizontal shearing stress, τ_{xy}, in the remote sections from the load indicated in Fig.9. The intensity of τ_{xy} increases toward the top surface of cracked sections, and its maximum value reaches about 2.5 times the value, $6M_{xy}/h^2$, in which M_{xy} is twisting moment, which is derived from the elementary plate bending theory. As the applied load moves away from a relevant cracked section, τ_{xy} related with twisting moment increases gradually but the other stress components except τ_{xy} decrease rapidly. Then, the maximum principal tensile stress, σ_{p2}, at the top surface of the cracked section will be given by

$$\sigma_{p2} \doteqdot 2.5 \frac{6M_{xy}}{h^2} \quad (2)$$

Fig.16 indicates a distribution of M_{xy} in the same one-way slab, as shown in Fig.15, subjected to two rear wheel loads with the intensity, 108 kN, respectively. Using the result from Fig.16 and eq.(2) under the assumption, h=17 cm, the predominant value of σ_{p2} will be in a range from 2.5 MN/m^2 to 3.5 MN/m^2 in an extensive region. Accordingly, this tensile stress may induce a new crack developing from the top surface toward the tip of a precedent flexural crack.

In ordinary bridge deck slabs meeting the Japanese code, such tensile stresses, σ_{p1} and σ_{p2}, possibly exceed the inherent tensile strength of concrete, particularly when considering impaired strength due to fatigue. Hence, the combined action of σ_{p1} and σ_{p2} alternately resulting from repetition of moving wheel loads will eventually induce full penetration of crack extending from the bottom surface of the slab to the top surface.

Finally, it should be mentioned that both compressive stresses in concrete at the top surface and tensile stresses in reinforcing bars almost never become greater than those derived from the conventional formula under moment calculated by the elementary plate bending theory, even if cracking progresses so severely that shear resistances of crack surfaces vanish and some cracks penetrating the entire depth exist. Then, it can be supposed that failure of concrete at the flexural compression side precedes the tensile fracture of reinforcing bars in actual bridge deck slabs.

Conclusion

It was found that deterioration of a reinforced concrete bridge deck slab under repetitions of both pulsating and moving loads proceeded through the following process: cracking patterns at the bottom surface of the slab were of a grid-like form; propagation of surface cracks ceased after a certain finite number of repetitions of the load; crack faces of concrete were rubbed together and were worn down by virtue of repetitions of moving loads, and slits with narrow openings were consequently formed in the cracked sections; the formation of such slits reduced the shearing rigidity of the slab associated with interlocking of the aggregate particles; and if rain water entered the cracked sections, the reductions of both flexural and shearing rigidities were remarkably accelerated making it possible to cause the slab surface to cave in and to collapse under the moderate load estimated in the design code.

On the other hand, three-dimensional stress analysis for the vicinities of cracks revealed the process of full penetration of cracks through the entire depth of the slabs. This process consisted of two stages: the first stage was the growth of flexural cracks occurring at the bottom surface of the slab beneath a wheel load, and the second stage was progression of twisting cracks occurring at the upper side of the cracked section of the first stage when the wheel load had moved away to a remote position.

Acknowledgement

The assistance of the Ministry of Construction of Japan in supplying the distressed deck slabs is gratefully acknowledged.

References

1. Y. Kakuta et al. Experimental Study on Fatigue Punching Shear Strength of Reinforced Concrete Slabs. CAJ Review of 28th General Meeting, held in Tokyo, May, 1974.
2. The Research Committee on Fatigue Design of Reinforced Concrete Slab. Fatigue Modes of Reinforced Concrete Deck Slabs and An Approach to Fatigue Design Thereof. Kansai Branch of the Japan Society of Civil Engineers, Osaka, 1977.
3. Y. Kakuta et al. Experimental Study on Punching Strength of Reinforced Concrete Slabs. Proc. of the Japan Society of Civil Engineers, No.229, 1974, pp.105-115.
4. H. Okamura et al. A Method of Numerical Analysis of Three-Dimensional Elastic Problems with Its Applications. Proc. of the Japan Society of Civil Engneers, No.199, 1972, pp.33-43.
5. H. Okamura et al. A Method of Three-Dimensional Analysis of Solid of Elasto-Plastic Property or of Nonuniform Elasticity. Proc. of the Japan Society of Civil Engineers, No.212, 1974, pp.11-24.